Available online at www.sciencedirect.com
ScienceDirect
Coordination Chemistry Reviews 252 (2008) 2395–2409
COORDINATION CHEMISTRY REVIEWS
www.elsevier.com/locate/ccr

Review

NMR: A good tool to ascertain σ-silane or σ-borane formulations?

Gilles Alcaraz, Sylviane Sabo-Etienne *

Laboratoire de Chimie de Coordination du CNRS, 205 route de Narbonne, 31077 Toulouse Cedex 04, France

Received 19 December 2007; accepted 10 February 2008
Available online 16 February 2008

Contents

Abstract

NMR has played a major role in the characterization of dihydrogen complexes and a number of polyhydrides have been reformulated as dihydrogen complexes on the basis of NMR data. If dihydrogen complexes remain the most widely studied class of σ-complexes, silane compounds are also well recognized as an important family of σ-complexes and more recently a few σ-borane compounds have been isolated. One important problem is the discrimination between a σ-formulation and the corresponding hydrido(silyl) or hydrido(boryl) oxidative addition product. In this review we will discuss key literature data on silane and borane complexes to illustrate the benefit gained by using multinuclear NMR spectroscopy to better define the structures and bonding modes. Our goal is also to help the reader to appreciate the limits of the method and to provide valuable insights into the problem of secondary interactions.

Keywords: NMR; Transition metals; σ-Complexes; Silanes; Boranes; Dihydrogen; Oxidative addition

1. Introduction

σ-Complexes can be defined as complexes incorporating a ligand in which a σ-H–E bond (E = H, B, C, Si, etc.) acts as a two-electron donor to the metal, resulting in a three-center bond (Fig. 1) [1].

They can be distinguished from the related class of agostic complexes by the fact that they display no other strong intramolecular interaction ("*not stabilized by a primary linkage such as in intramolecular σ-bond interactions*, *commonly known as agostic interactions*" as quoted by Kubas in his book [1]). σ-Complexes are very often considered as intermediates in the process of oxidative addition of H–E and its microreverse reductive elimination step (Fig. 2). These different bonding schemes portray a broad aspect of chemistry which is especially relevant in various catalytic reactions (hydrogenation,

* Corresponding author. Tel.: +33 5 61 33 31 77; fax: +33 5 61 55 30 03.
E-mail address: sylviane.sabo@lcc-toulouse.fr (S. Sabo-Etienne).

0010-8545/$ – see front matter © 2008 Elsevier B.V. All rights reserved.
doi:10.1016/j.ccr.2008.02.006

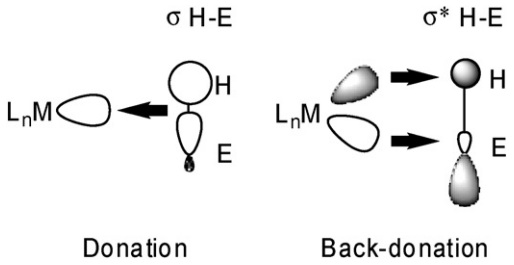

Fig. 1. Classical model of Chatt, Dewar and Duncanson for the σ-EH coordination mode.

hydrosilylation, hydroboration, etc.). It is thus important to gain knowledge on the activation process of the H–E bond [2,3].

After the seminal paper by Kubas et al. in 1984 of the first σ-dihydrogen complex [4], several groups have worked in finding good tools to ascertain a σ-coordination versus the formation of the corresponding dihydride [5–10]. It became rapidly apparent that combination of several techniques was needed to really get a good bonding picture. X-ray structure determination is of course a method of choice but it remains difficult to ascertain hydrogen location by this technique. Recent years have seen a tremendous progress of DFT calculations and it is now more and more common to combine X-ray and DFT data to better locate hydrogen atoms [11]. Neutron data are highly desirable but it is not easy to grow crystals for such measurements and the equipment is not of course available in many places [12,13]. It is also often difficult to get valuable information from IR data due to intensity problems and to the presence of other ligands that may hide some interesting modes. Indeed, NMR spectroscopy has played a major role in the establishment of σ-coordination, especially for the dihydrogen family [1,10]. Two methods were particularly useful for the estimation of the H–H distance: partial deuteration of the compound to determine the corresponding J_{HD} coupling constant and T_{1min} measurements. Both data give access to the H–H distance thanks to empirical formula. We will not detail these aspects that will be covered in the Morris review within this special CCR issue.

We focus our review on the properties of two other important classes of σ-complexes: σ-silane and σ-borane complexes. Dihydrogen activation is simple (it was not the case 25 years ago!) as dihydrogen has two identical atoms, whereas in silanes and boranes the Si–H and B–H bonds are polarized and the heteroatom bears substituents that will affect the σ-coordination. It is thus interesting to combine data on these two families. The two heteroatoms ^{29}Si (I = 1/2, 4.7%) and ^{11}B (I = 3/2, 80.2%) can be monitored by NMR which can offer complementary information. This review is intended to analyze the literature where

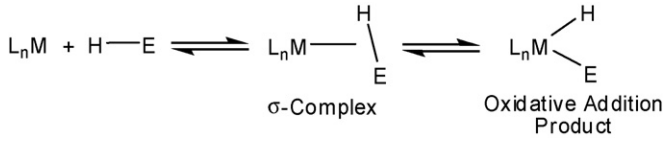

Fig. 2. Process of oxidative addition of H-E and its microreverse reductive elimination step.

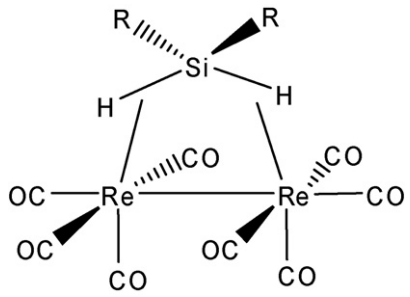

Fig. 3. $Ph_2SiH_2Re_2(CO)_8$ silane σ-complex [16].

NMR had a significant impact in the understanding of the activation degree of the H–Si and H–B bonds. The factors that allow distinguishing a σ-formulation from the corresponding product of oxidative addition will be particularly analyzed. The first section will summarize some key features in silane chemistry, whereas in the following section devoted to borane activation, we will be more comprehensive as this field is much more recent.

2. σ-Silane complexes

There is a close relationship between H–Si and H–H complexes. However, there is one main difference as a result of the H–Si bond asymmetry with an important change in size and electronegativity between the two atoms. In σ-silane complexes, the hydrogen is close to the metal with M–H–Si angles near 90°. Silicon substituents with various steric and electronic properties can of course modify the σ-interaction. Moreover, silicon is known for being a hypervalent element. This property leads to the formation of additional interactions that will also modify the σ-coordination [14,15].

Historically, the paper published by Hoyano et al. should be recognized as the first report of a σ-complex [16]. As early as 1969, the authors on the basis of X-ray, IR, mass spectrum and NMR data described the complex $Ph_2SiH_2Re_2(CO)_8$ shown in Fig. 3 in the following terms: "each silicon–hydrogen bond functions as a two-electron donor to rhenium, effectively taking the place of a carbonyl group; the interaction could be described as a three-centre, two-electron bond with the two electrons supplied by the original Si–H bond." The complex was characterized by a high-field signal at $\delta - 9.56$. By changing the phenyl substituents to methyl they observed that the methyl proton resonance appeared as a triplet at $\delta - 1.13$ (J = 1.5 Hz) which collapsed to a singlet upon irradiation of the broad signal at $\delta - 10.56$. In 1969, NMR was still at an early stage of development but it is impressive to see that the authors had already such an accurate bonding description.

We had then to wait until the 1980s to see the development of σ-silane chemistry. In 1982, Corriu and co-workers reported one of the first NMR study on manganese complexes including ^{29}Si NMR data and $J_{Si–H}$ measurements for a variety of silanes [17]. For example, the complex $Cp'Mn(\eta^2\text{-}HSiPh_3)(CO)_2$ was characterized by a ^{29}Si NMR resonance at δ 18.5, shifted downfield by *ca.* 40 ppm from the parent silane. The $J_{Si–H}$ value of 65 Hz in the complex indicated a significant Si–H bond

interaction, by comparison to a value of 198 Hz in the parent silane. Schubert's group brought an important contribution on a series of stretched group 7 complexes and the main data on σ-silane chemistry were summarized in 1990 by Schubert [18].

Since that time, the same problems remain, and it is still difficult to discriminate a σ-silane formulation from the corresponding hydrido(silyl) species on the only basis of ^{29}Si and ^{1}H NMR chemical shift. This is well evidenced by examining all the data compiled in the impressive review published in 1999 by Corey and Braddock-Wilking [19]. Si–H resonance of the free silane will generally appear between 4 and 5.5 ppm in the ^{1}H NMR spectrum. Addition of a silane to a transition metal complex and formation of a new complex incorporating the silicon fragment can thus be monitored by the disappearance of that signal. Formation of the corresponding hydrido(silyl) or σ-silane complex will lead to a resonance in the negative high-field region, but unfortunately, the overlap for these two formulations is important and the values are highly influenced by the ligands on the metal and the substituents on silicon. ^{29}Si NMR is now much easier to record, thanks in particular to the accessibility of NMR machines at higher field and to indirect methods such as INEPT or HMBC sequences. However, reports on ^{29}Si NMR data are still limited. A downfield shift from the value of the free silane is generally observed for transition metal complexes incorporating a silicon group. Substituents at Si have an important effect on the ^{29}Si chemical shifts with an important downfield shift for electron-withdrawing groups such as Cl. Recording of the ^{29}Si chemical shifts is a good tool to discard a silylene formulation, the ^{29}Si NMR signal appearing at a much lower field (>100 ppm) [19]. However, there is at least one exception found in the dinuclear ruthenium complex $Ru_2H_4(\eta^2{:}\eta^2{:}\eta^2{:}\eta^2\text{-}SiH_4)(PR_3)_4$ (R = ^{i}Pr, Cy) which displays a very downfield chemical shift value of 290 ppm. In fact, the bridging SiH_4 ligand is bonded to two ruthenium atoms through multiple σ-Si–H interactions as shown by multinuclear NMR, X-ray and DFT studies [20,21].

One can gain a lot of information from coupling constant values, but again the data should be analyzed very carefully. There are very few data on J_{MSi} coupling constants and a rather large range is observed for ^{183}W, ^{103}Rh or ^{195}Pt species. The $^{1}J_{SiH}$ values in free silanes are around 200 Hz but extreme values are found from 190 Hz in $HSiMe_3$ to 370.6 Hz in $HSiCl_3$ due in part to an increase in the s character in the Si–H bond. For complexes displaying $^{2}J_{SiH}$ values below 10 Hz, a Si–H interaction can be excluded, and a hydrido(silyl) formulation is likely. Similarly, values higher than 65 Hz are a good criterion to ascertain a σ-silane formulation. In between, it is essential to combine additional data (IR, X-ray, DFT) to discriminate the two bonding situations. The intermediate range has varied over the years as more and more examples have been found and have shown that the interpretation of J_{SiH} values can be quite difficult, especially for silanes with electron-withdrawing substituents. Fluxional processes are often observed in hydrido(silyl) and σ-silane complexes which might also add complexity in the analysis of the bonding nature.

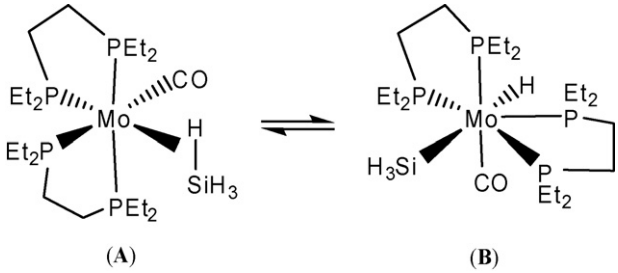

Fig. 4. σ-SiH_4 complex $Mo(\eta^2\text{-}HSiH_3)(CO)(depe)_2$ (**A**) in tautomeric equilibrium with $MoH(SiH_3)(CO)(depe)_2$ (**B**) [22].

In order to illustrate these NMR features, we have selected a few examples among the three different classes: σ-silane, hydrido(silyl) and ambiguous systems.

2.1. Tautomeric equilibrium in a molybdenum complex

In 1995, Kubas et al. reported the first transition metal σ-SiH_4 complex $Mo(\eta^2\text{-}HSiH_3)(CO)(depe)_2$ (**A**) (depe = $Et_2PC_2H_4PEt_2$) in tautomeric equilibrium with the corresponding hydridosilyl species $MoH(SiH_3)(CO)(depe)_2$ (**B**) (Fig. 4) [22]. The σ-SiH_4 complex **A** is characterized by a broad hydride signal at $\delta - 8.23$ displaying a J_{SiH} value of 35 Hz in the $^{1}H\{^{31}P\}$ NMR spectrum, whereas the hydridosilyl isomer **B** presents a hydride quintet at $\delta - 7.58$ with no visible silicon satellites upon phosphorus decoupling. The tautomeric equilibrium is demonstrated by variable temperature ^{1}H and ^{31}P NMR measurements. The X-ray structure of $Mo(\eta^2\text{-}HSiH_3)(CO)(^{i}Bu_2PC_2H_4P^{i}Bu_2)_2$ analogous to **A** was also reported. Unfortunately the hydride could not be located, but the geometry of the central core MoP_4CSi is very similar to that in the related compound $Mo(\eta^2\text{-}HSiH_2Ph)(CO)(Et_2PC_2H_4PEt_2)_2$ in which all the hydrogen atoms were located. It is interesting to note that an analogous σ-germane complex was also structurally characterized.

2.2. Silane manganese complexes

After the paper by Jetz and Graham in 1971 on the synthesis of two manganese complexes $CpMn(CO)_2\{HSiPh_3\}$ and $CpMn(CO)_2\{HSiCl_3\}$ [23], more information has been gained on a series of complexes of the type $Cp'Mn(CO)_2\{HSiR_3\}$ (with $Cp' = C_5H_5$, C_5Me_5, C_5H_4Me and $HSiR_3 = HSiHPh_2$, $HSiHPh(C_{10}H_7)$, $HSiFPh_2$, $HSiPh_3$, $HSiCl_3$, $HSiPh_2SiHPh_2$). All the complexes display in the hydride region of the ^{1}H NMR spectrum one signal close to $\delta - 11$. Silicon satellites could be measured giving rise to a rather narrow range for the J_{Si-H} values, 55–65 Hz, whereas the corresponding ^{29}Si NMR resonances are spread between $\delta - 2$ to $\delta + 55$ as a result of various silicon substituents (see Table 1). Complementary data came from PES, IR, X-ray and even neutron structure determination (d_{Si-H} = 1.802(5) Å for $Cp'Mn(CO)_2\{HSiPh_2F\}$) leading to a good agreement for a σ-silane formulation.

However, the structure for the complexes resulting from the activation of $HSiCl_3$ remained under debate and led to two correspondences in 2003 by Nikonov [31] and Licht-

Table 1
Selected data for $Cp^RMn(CO)_2\{HSiR_3\}$ complexes

Complex	δ ^{1}H	J_{SiH}	δ ^{29}Si	Ref.
$MeCpMn(CO)_2\{HSiHPh_2\}$	−11.5	63.5	13.5	[24–27]
$Cp^*Mn(CO)_2\{HSiHPh_2\}$	−11.2	65.4	18.2	[24,26]
$MeCpMn(CO)_2\{HSiHPhC_{10}H_7\}$	−1.23	69	7.5	[17]
$MeCpMn(CO)_2\{HSiPh_3\}$	−11.44	64.7	18.5	[17,23]
$MeCpMn(CO)_2\{HSiPh_2SiHPh_2\}$	−10.71	57	−2.62	[28]
$MeCpMn(CO)_2\{HSiPh_2F\}$	−11.0			[24,29]
$CpMn(CO)_2\{HSiCl_3\}$	−9.70			[23]
$MeCpMn(CO)_2\{HSiCl_3\}$		54.8	54.9	[24,30]

$Cp = C_5H_5$; $MeCp = C_5H_4Me$; $Cp^* = C_5Me_5$.

enberger [32]. Recently, Scherer et al. reinvestigated these systems [33]. On the basis of charge density analysis and T_1 measurements to estimate M–H distances, they concluded on a similar (η^2-$HSiR_3$) bonding mode within the three complexes $MeCpMn(CO)_2\{HSiHPh_2\}$, $MeCpMn(CO)_2\{HSiFPh_2\}$ and $MeCpMn(CO)_2\{HSiCl_3\}$. Certainly, the introduction of more electronegative substituents pushes the activation to a more pronounced asymmetric oxidative addition stage. The results are a good illustration of an activation process through a continuum and for which the borders are difficult to delineate.

2.3. The ruthenium $RuH_3(SiR_3)L_2L'$ series

A series of ruthenium complexes of general formula $RuH_3(SiR_3)L_2L'$ can be isolated from the reactions of dihydride complexes with a variety of monosilanes $HSiR_3$ (R = alkyl, aryl, alkoxy or halogen) [34–42]. They all display similar NMR features, no matter what the other ligands L and L′ around the metal center are, with one hydride resonance at all temperatures. Analysis of $J_{Si–H}$ coupling constant values was quite difficult in view of the different substituents leading to some controversy on the formulation of this family of complexes [14,15]. Recent progress made on theoretical calculations of NMR parameters should offer, in the future, complementary information to X-ray and DFT data [32].

2.4. Disilane ruthenium complexes

The coordination of disilanes to the bis(dihydrogen) complex $RuH_2(H_2)_2(PCy_3)_2$ led to the synthesis of a series of complexes of general formula $[RuH_2\{(\eta^2\text{-}HSiMe_2)_2X\}(PCy_3)_2]$ (Fig. 5) [43]. X-ray structures were obtained in particular for $X = C_6H_4$,

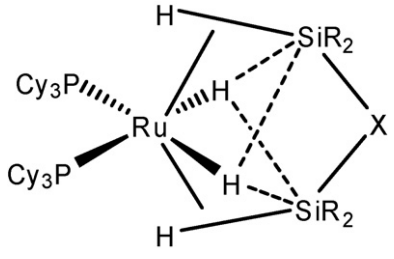

Fig. 5. SISHA interactions between hydrides and silicon atoms in disilane complexes $[RuH_2\{(\eta^2\text{-}HSiMe_2)_2X\}(PCy_3)_2]$.

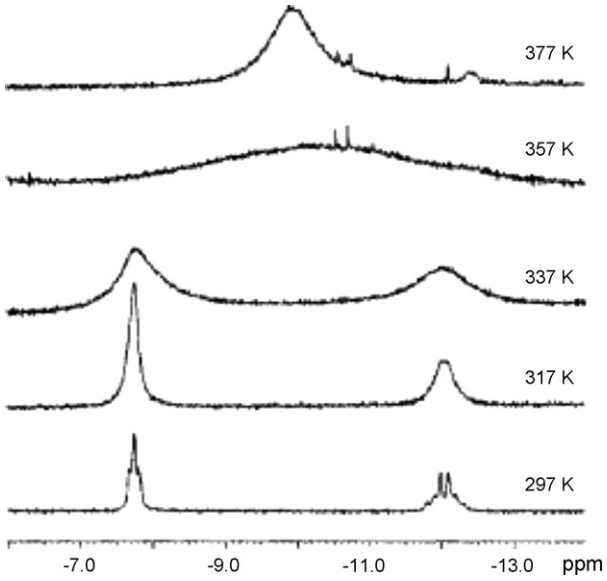

Fig. 6. ^{1}H NMR spectra at various temperatures of $[RuH_2\{(\eta^2\text{-}HSiMe_2)_2(C_6H_4)\}(PCy_3)_2]$.

$(CH_2)_2$ and $OSiMe_2O$ [44]. The measurements at low temperature allowed a very good location of the hydrogen atoms, ascertained by DFT calculations [44]. They display the same overall structure, a distorted octahedral with two *cis* phosphines and the disilane ligand bonded to the ruthenium through two σ-Si–H bonds (*ca.* 1.8 Å) in a *trans* position. The *cis* position of these bulky phosphines was quite unexpected and analysis of all the data (X-ray, NMR, IR and DFT) led us to conclude to the importance of secondary interactions between the silicon atoms and the classical hydrides, named SISHA interactions (see Section 2.5) [14,15,45]. These secondary interactions were in particular characterized by Si···H distances around 2.2 Å, much shorter than the sum of the van der Waals radii (3.4 Å for hydrogen and silicon).

These three complexes display similar NMR data. The single line in the range 45–51 ppm in the $^{31}P\{^1H\}$ NMR spectrum is in agreement with two equivalent phosphines. At room temperature, the ^{1}H NMR signal of the starting disilane close to $\delta + 5$ had disappeared, and two signals of equal intensity were observed in the hydride region of the spectrum: one triplet near $\delta - 8$ assigned to the σ-Si–H and an AA′XX′ resonance near $\delta - 12$ for the two classical hydrides. Similarly to what is observed for dihydrogen complexes, a reduced J_{HP} value was observed within the triplet in agreement with a σ-formulation. Coalescence was achieved at temperatures higher than 333 K leading to a broad resonance near $\delta - 10$ (Fig. 6).

These exchange processes are characterized by a barrier close to 65 kJ mol^{-1}. Deuterium incorporation was equally observed on the two hydride sites in agreement with a rather easy exchange process between the two types of hydrogens. The absence of any dihydrogen ligand in all of the new complexes was confirmed by T_1 measurements giving T_{1min} values higher than 140 ms for the two signals. The $^{29}Si\{^{31}P\}$ INEPT spectra showed a doublet with J_{SiH} values in the range 65–82 Hz, representing a significant reduction from the values

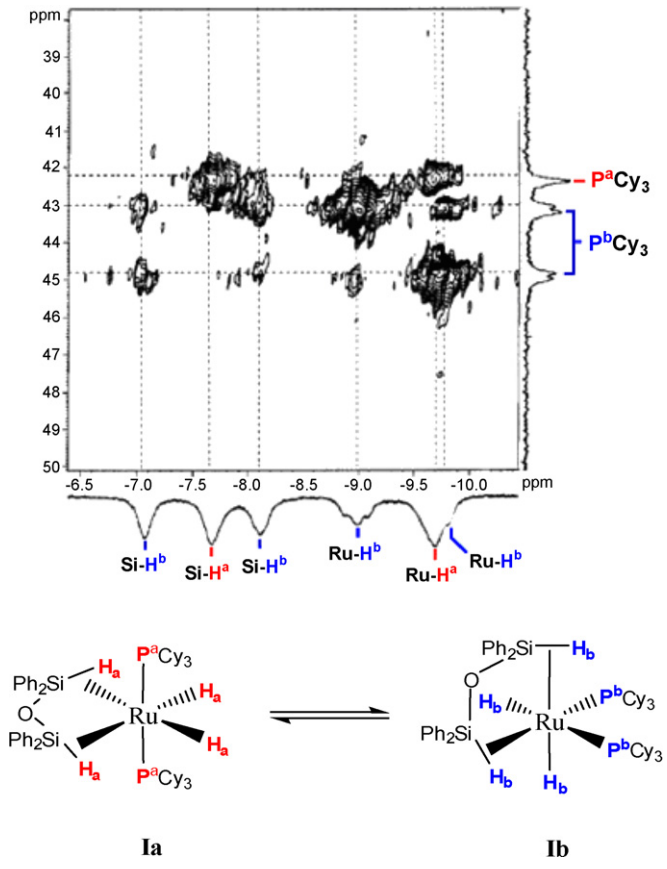

Fig. 7. [^{1}H, ^{31}P] HMQC spectrum of [$RuH_2\{(\eta^2\text{-}HSiPh_2)_2O\}(PCy_3)_2$] at 183 K showing the two isomers **Ia** and **Ib**.

for the free disilanes (179–204 Hz) as a result of σ-coordination and stretching of the Si–H bonds. In this series of disilane complexes, the J_{Si-P} values were found close to 8 Hz. Such small values are typical for σ-silane complexes. Higher values can be observed in the case of agostic complexes (37 Hz for the β-agostic complex Cp*Ru{C(HSiMe$_2$)=CPh$_2$}(PR$_3$) [46]), whereas important variations depending on the P–M–Si angle are observed for silyl complexes (164 Hz in a tetrasilyl palladium complex with a P–Pd–Si angle of 175.5(1)° [47]).

When a short spacer bridges the two silicon atoms such as in the case of disiloxane (X = O) or disilazane (X = NH), the corresponding ruthenium complexes [$RuH_2\{(\eta^2\text{-}HSiR_2)_2X\}(PCy_3)_2$] display different NMR, X-ray as well as DFT data [44,45,48]. As a result of a steric constraint, the compounds are now characterized by a *cis* disposition of the two (η^2-H–Si) ligands. The disiloxane and disilazane complexes display similar NMR spectra. We will only comment the data for the disiloxane complex [$RuH_2\{(\eta^2\text{-}HSiPh_2)_2O\}(PCy_3)_2$] which is the only one displaying an equilibrium between two isomers as shown by multinuclear NMR experiments. At room temperature one broad signal in the hydride ^{1}H NMR region is observed at $\delta -8.79$. A first decoalescence at 273 K led to a broad singlet at $\delta -7.77$ and a broad triplet at $\delta -9.57$ (J_{HP} = 45 Hz) followed by a second decoalescence at 213 K leading finally to the observation of five broad signals between $\delta -7$ and $\delta -10$ in a 1:1:1:1:2 ratio. The ^{31}P NMR spectrum showed one signal at δ 45 at room temperature which transformed into a singlet at δ 42.4 and an AB pattern at δ 44.9 and δ 43.1 with J_{PP} of 28 Hz. All the data were consistent with the formation of two isomers as identified in particular by [^{1}H, ^{31}P] HMQC and EXSY experiments (Fig. 7). The symmetrical isomer **Ia** corresponds to a *trans* arrangement of the phosphines whereas in the asymmetrical isomer **Ib**, the phosphines adopt a *cis* disposition and all the hydrogen atoms around the ruthenium are inequivalent [45]. In the case of the analogous disiloxane and disilazane complexes with methyl substituents on silicon, [$RuH_2\{(\eta^2\text{-}HSiMe_2)_2X\}(PCy_3)_2$], the symmetrical isomer **a** was not observed. The structure of [$RuH_2\{(\eta^2\text{-}HSiMe_2)_2NH\}(PCy_3)_2$] was confirmed by X-ray diffraction. It is noteworthy that the choice of the functional for DFT calculations was crucial. Indeed, a major discrepancy with X-ray data was observed when using B3LYP instead of B3PW91 [48].

2.5. Secondary Si···H interactions (SISHA)

The only case for which it was possible to identify a Secondary Interaction between Silicon and Hydrogen Atoms (SISHA) by NMR was on the complexes $RuH(\eta^2\text{-}HSiR_3)\{(\eta^3\text{-}C_6H_8)PCy_2\}(PCy_3)$ (SiR_3 = $SiEt_3$, $SiMe_2Et$ and $SiMe_2Cl$) [42,49]. We have in this series two different phosphines and there is no hydride exchange.

In $RuH(\eta^2\text{-}HSiMe_2Cl)\{(\eta^3\text{-}C_6H_8)PCy_2\}(PCy_3)$ for example, the two hydrides resonate at $\delta -9.06$ (t) and $\delta -11.98$ (dd) and an AB pattern (δ 83.9 and δ 68.8, J_{PP} = 18.6 Hz) is observed in the ^{31}P{^{1}H} spectrum. A 1D HMQC ^{29}Si–^{1}H{^{31}P} experiment shows two doublets in the high-field region with J_{SiH} values of 37.3 and 24.1 Hz (Fig. 8). The coupling of the two different hydrides with silicon is noticeably different (ΔJ_{SiH} = 13 Hz) but surprisingly almost no change was recorded for the two analogous complexes with $HSiEt_3$ or $HSiMe_2Et$. A rather significant change on the Si–H bond activation was expected at least between $HSiMe_2Cl$ and $HSiMe_2Et$ because of the chloride substituent. Again, we see here that a direct interpretation of the J_{SiH} value for the description of the bonding mode of the silane should be used with caution.

3. σ-Borane compounds

B–H activation is well known and largely dominated by the use of borohydride compounds (predominantly BH_4^-) and borane-Lewis base adducts. We have excluded here the chemistry of boryl, borylene and borane-Lewis base complexes [50–57]. The chemistry of *true* σ-B–H complexes started in 1996 when Hartwig et al. found an elegant entry by using neutral trivalent boranes [58]. The authors described the complexes $Cp_2Ti(\eta^2\text{-}HBcat)_2$ and $Cp_2Ti(\eta^2\text{-}HBcat\text{-}4\text{-}Me)_2$ as the σ-B–H complexation of two catecholborane molecules to a 14-electron Cp_2Ti fragment. Until today, a limited number of M-(σ-B–H) complexes (M = Ti, Nb, Mn, Re, Ni and Ru) have been reported.

The close relationship between H–Si and H–H complexes can also be extended to H–B complexes. As in the case of silanes, the nature of the boron substituents is important. They can modify the Lewis acid properties of the borane and in partic-

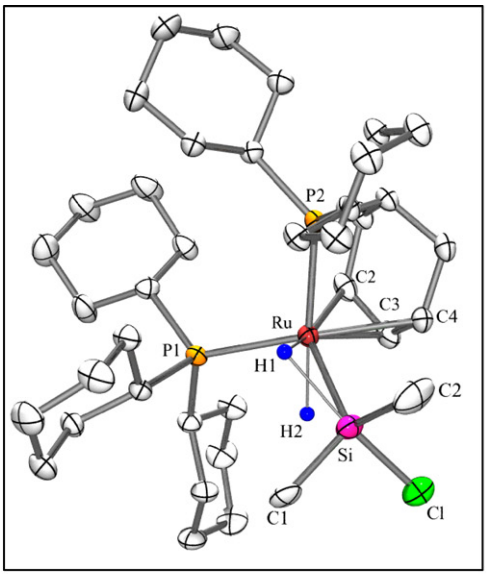

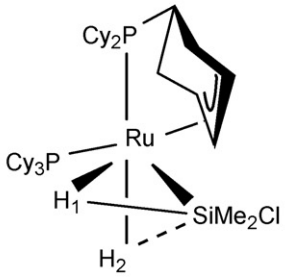

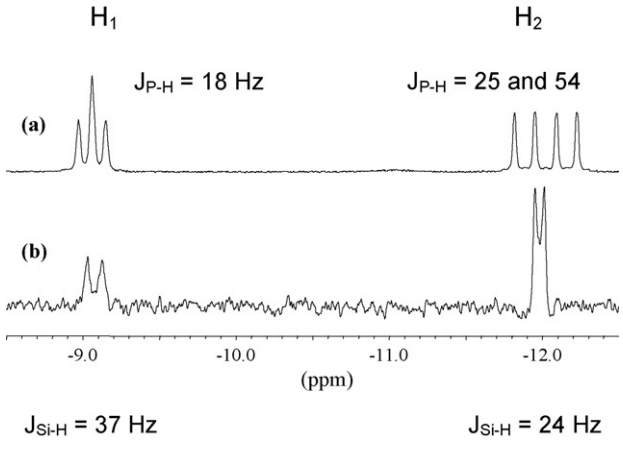

Fig. 8. RuH(η^2-HSiMe$_2$Cl){(η^3-C$_6$H$_8$)PCy$_2$}(PCy$_3$). Top: X-ray crystal structure. Down: (a) ^{1}H NMR spectrum and (b) 1D HMQC ^{29}Si–^{1}H{^{31}P} NMR spectrum in the hydride region showing the different coupling constants.

ular favour a σ-borane over a hydrido(boryl) formulation. The presence of an empty p orbital on boron represents an additional contribution to the classical model of Chatt, Dewar and Duncanson (Fig. 9). As in silane chemistry, it remains difficult to assign a correct formulation on the only basis of ^{11}B and ^{1}H NMR. Fig. 10 shows the various structures that can be adopted when a borane is added to a metal hydride fragment. Representative examples will be described in the following sections.

Most of the σ-B–H complexes involve the complexation of catecholborane (HBcat) or pinacolborane (HBpin) that are

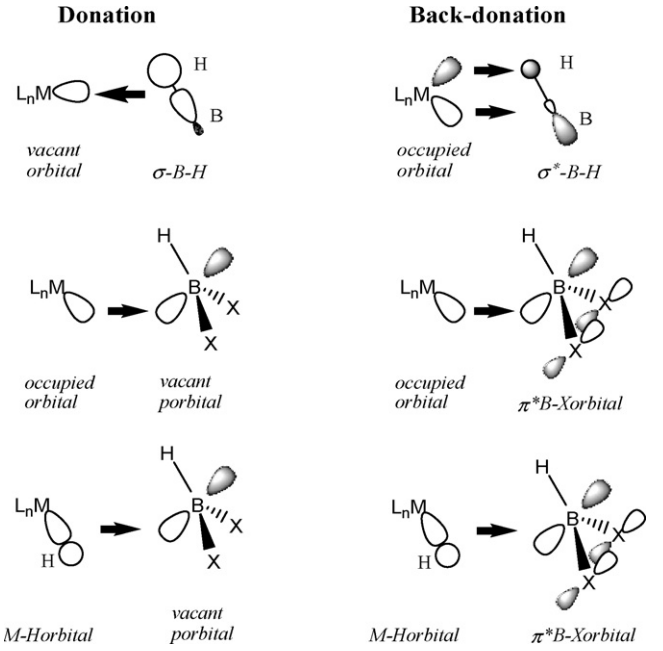

Fig. 9. Additional contribution of the empty p orbital on boron to the classical model of Chatt, Dewar and Duncanson in a σ-BH complex.

monomeric species in solution. In these cases, downfield shifts (>40 ppm) are observed by ^{11}B NMR between the starting borane and the metal complex as a result of borane incorporation. The case of σ-dialkylborane complexes is less obvious. The ^{11}B NMR resonances are rather located downfield with a chemical shift depending on the nature of the metal. The values are not directly comparable with the chemical shifts of the corresponding free dialkylboranes. Most of them are dimeric species and display chemical shifts around 20–30 ppm. When monomeric, the ^{11}B NMR resonances of free dialkylboranes are expected to be much more deshielded [59]. Dimesitylborane was characterized as a dimer by neutron and X-ray diffraction. In solution, equilibrium with the monomer form was evidenced by the two broad ^{11}B NMR signals at δ 25.9 (dimer) and δ 73.3 (monomer) [60]. A similar trend is generally observed in a smaller magnitude for the ^{11}B NMR signals of metal–boryl complexes. They are located downfield of those of free boranes whereas borohydrides are located upfield.

The B–H bond of free monomeric or dimeric boranes is generally characterized by a positive chemical shift ^{1}H NMR signal, appearing as a poorly resolved quartet due to the quadrupolar boron atom. Sharpening of the signal is observed upon boron decoupling. When incorporated into a metal complex, the signal of the σ-B–H remains broad but it is strongly shielded. The hydrogen atom shows a hydridic character and displays a negative chemical shift ($-5.4 < \delta < -17.1$). However, the assignment of a bonding mode by a simple analysis of the chemical shift values is impossible as similar ranges are observed for hydrido(boryl) and borohydride complexes.

Analysis of coupling constant values brings normally useful information but unfortunately, data are extremely limited in σ-borane chemistry. The σ-B–H resonance signal is generally too

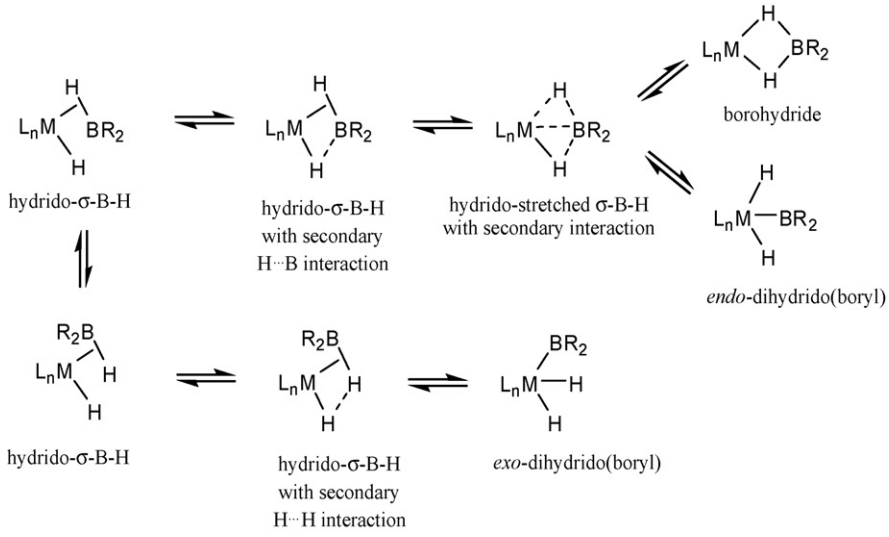

Fig. 10. Possible coordination modes for boranes to a metal hydride fragment.

broad to allow J_{BH} measurements due to the coupling with the quadrupolar ^{11}B atom [61–63]. ^{1}H NMR with ^{11}B decoupling leads to a sharper signal but the coupling information is lost. This trend is shared by most of the reported σ-B–H complexes and by borohydride complexes. It becomes debatable in the case of hydrido(boryl) complexes. The presence and the magnitude of a potential secondary interaction between a hydride and the boron of a boryl complex can also be responsible of the broadening of the hydride signal in ^{1}H NMR.

In the following sections, we will exhaustively present key NMR features of all the σ-B–H complexes so far reported. Whenever possible, we will compare them with some hydrido(boryl) or borohydride species for a better understanding of the σ-coordination mode.

3.1. Titanium complexes

In 1996, Hartwig et al. reported the first transition metal σ-BH complexes $Cp_2Ti(\eta^2\text{-HBcat})_2$ (**A$_1$**) and $Cp_2Ti(\eta^2\text{-HBcat-4-Me})_2$ (**A$_4$**) followed by a series of analogous Ti complexes incorporating substituted catecholboranes [58,64] (Fig. 11). They have been fully characterized by X-ray, infrared, multinuclear NMR spectroscopy and their structure has been rationalized by theoretical calculations. In the case of **A$_1$**, the X-ray analysis showed a Ti–H distance of 1.25(3) Å and a Ti–B distance of 2.335(5) Å, longer than that of metallocene boryl complexes [65,66]. All the data are consistent with the presence of a d^2 Ti(II) center.

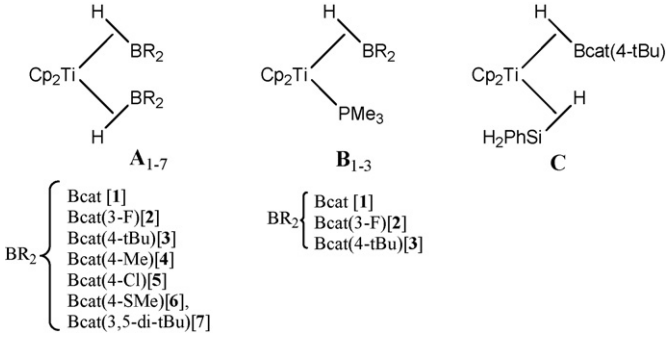

Fig. 11. σ-BH titanocene complexes incorporating substituted catecholboranes (**A**, **B** and **C**).

Complexes **A$_{1–7}$** exhibit similar spectroscopic characteristics: (i) a broad ^{11}B NMR signal between 45 and 46.3 ppm moderately deshielded with respect to the starting catecholboranes, and (ii) broad ^{1}H NMR hydride resonances between −5.85 and −5.37 ppm which sharpen upon boron decoupling. They are strongly shielded compared to the B–H resonances of the parent catecholboranes (see Table 2). The two hydride resonances due to the different orientations of the substituted catechol ligand are not resolved except in the case of complex **A$_7$** containing two bulky *tert*-butyl groups per catechol [64]. Interestingly, **A$_3$** is a highly active catalyst for the hydroboration of vinylarenes [67].

Compounds **B$_{1–3}$** (Fig. 11) were obtained from **A** by a redistribution reaction with $Cp_2Ti(PMe_3)_2$ or directly by exchange of one catecholborane ligand with PMe_3 [64,68]. It is noteworthy that σ-complex chemistry is largely dominated by substitution reactions [1]. Kinetic studies conducted with **A** indicated a zero order dependence in both borane and PMe_3 concentrations. The mechanism involves an initial dissociation step of the catecholborane ligand followed by a rapid association of the phosphine. The measured rate constants suggest that more electron-withdrawing substituents on the catechol moiety decrease the rate of substitution [64]. The X-ray analysis in the case of **B$_2$** showed as in **A$_1$** a Ti–H–B angle of 100°. The measured Ti–B distance of 2.267(6) Å in **B$_2$** is too long for a metallocene–boryl complex but is slightly shorter than that in **A$_1$**. A same trend is observed for the Ti–H bond with a length of 1.61(5) Å (1.74(4) Å in **A$_1$**). On the contrary, the B–H bond length of 1.35(5) Å is slightly longer than that in **A$_1$** (1.25(3) Å) and the angle between the midpoint of the B–H bond, Ti and P is 89.3°, thus larger than in **A$_1$** (81°). This angle is still in the range of L–M–L angles measured in d^2 Cp_2ML_2 compounds.

Table 2
NMR data on titanium complexes

	Complexes										
	$\mathbf{A_1}$	$\mathbf{A_2}$	$\mathbf{A_3}$	$\mathbf{A_4}$	$\mathbf{A_5}$	$\mathbf{A_6}$	$\mathbf{A_7}$	$\mathbf{B_1}$	$\mathbf{B_2}$	$\mathbf{B_3}$
^{11}B NMR, δ ($\Delta\delta$) (ppm)	+45 (+16)	+45.7 (+16.5)	+46.0 (+16.6)	+45.8 (+15.5)	+45.8 (+15.6)	+45.7 (+16.2)	+46.3 (+16.5)	+64.2 (+35.2)	+64.9 (+35.7)	+64.0 (+34.6)
^{1}H NMR, δ ($\Delta\delta$) (ppm)	−5.85 (−10.15)	−5.80 (−10.2)	−5.67 (−10.07)	−5.70 (−9.45)	−5.80 (−10.10)	−5.84 (−10.33)	−5.37, −6.15 (−9.67, −10.45)	−9.8 (−14.1)	−9.4 (−13.8)	−9.7 (−14.1)

These data are in agreement with a more advanced oxidative addition process in $\mathbf{B_2}$ compared to $\mathbf{A_1}$ as a result of the presence of PMe_3, a more basic ligand leading to a more efficient back-donation process to the borane.

The $^{31}P\{^1H\}$ NMR spectra of $\mathbf{B_{1–3}}$ consist in sharp singlets around δ 29 and no information is gained with respect to the coordination mode of the borane. The ^{11}B NMR data testify the borane incorporation in the complex. The borohydride coordination mode can be excluded as such a mode would exhibit a resonance located upfield to those of the free boranes. The spectra of compounds $\mathbf{B_{1–3}}$ contain a single resonance around δ 64 located downfield of those of the free catecholboranes and of the parent complexes $\mathbf{A_{1–3}}$ (see Table 2).

The most relevant information is obtained from the ^{1}H NMR analysis. The spectra of complexes $\mathbf{B_{1–3}}$ display a broad signal at *ca.* $\delta - 9.5$ located upfield of those of the free catecholboranes and parent complexes $\mathbf{A_{1–3}}$. In ^{1}H NMR, the analysis of the coupling constant values and their comparison with those of phosphine containing hydrido(boryl) complexes are quite informative. For example, in the case of the hydrido(boryl) complexes Cp*IrH(Bcat)(PMe_3) [69] and RhHCl(Bcat)(P^iPr_3)$_2$ [13,70] the hydride displays a sharp doublet with a $^2J_{PH}$ coupling constant of 29 Hz and 14 Hz, respectively. Their ^{11}B NMR spectra show a signal moderately deshielded (δ 35.98 ($\Delta\delta + 6$) and δ 37.7 ($\Delta\delta + 8$), respectively) compared to the resonance of free catecholborane but upfield of compounds $\mathbf{B_{1–3}}$ ($-29 < \Delta\delta < -26$). In $\mathbf{B_{1–3}}$, the broad hydride signal in ^{1}H NMR sharpens upon ^{11}B decoupling and the absence of any measurable J_{PH} coupling constant excludes a hydrido(boryl) coordination mode and reveals the B–H connectivity in agreement with a σ-borane coordination. Overall, the ^{11}B and ^{1}H NMR data for $\mathbf{B_{1–3}}$ illustrate the modification of the metal–ligand electron density transfer with respect to complexes $\mathbf{A_{1–3}}$.

Compound **C** (Fig. 11) was also prepared in 39% isolated yield from $\mathbf{A_3}$ by substitution reaction of one H–B(cat-4-tBu) ligand at −5 °C in toluene in the presence of a slight excess of phenylsilane. **C** was identified as an unusual mixed (σ-borane)(σ-silane) complex [64]. The ^{11}B NMR spectrum exhibits a signal at δ 37 slightly downfield of free H–B(cat-4-tBu) ($\Delta\delta + 7.7$) but upfield of that of $\mathbf{A_3}$ ($\Delta\delta - 9$) and $\mathbf{B_3}$ ($\Delta\delta - 27$ ppm) implying a significant contribution of the silyl(dihydroborate) form $Cp_2Ti(SiH_2Ph)[(\mu\text{-}H)_2Bcat(4\text{-}tBu)]$ to the overall structure. The hydride signals in **C** are not averaged in the ^{1}H NMR at −30 °C and the spectrum displays two hydride broad signals at $\delta - 6.79$ and $\delta - 4.99$ that sharpen upon ^{11}B decoupling. They were respectively assigned to σ-Si–H and σ-B–H. The *head-to-tail*-disposition of the σ-silane and the σ-borane is demonstrated by NOESY experiment. At −80 °C, a NOE interaction between the σ-B–H and the σ-Si–H is observed as well as between the σ-Si–H and the two uncoordinated hydrogen atoms of the phenylsilane, but not between the σ-B–H and the two uncoordinated hydrogen atoms of the phenylsilane. The ^{2}H NMR spectrum of $Cp_2Ti(HBcat)(PhSiH_3)$ at −30 °C indicated that H/D exchange between the B–H and the three Si–H bonds took place on the laboratory time scale. This corroborates the substantial borohydride character of **C** since metallocene borohydride complexes are known to

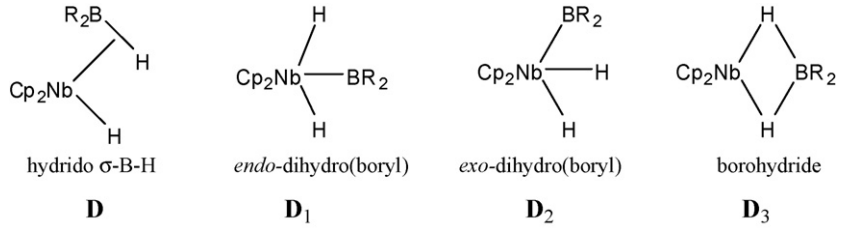

Fig. 12. Possible coordination modes of niobium complexes incorporating disubstituted boranes (**D**).

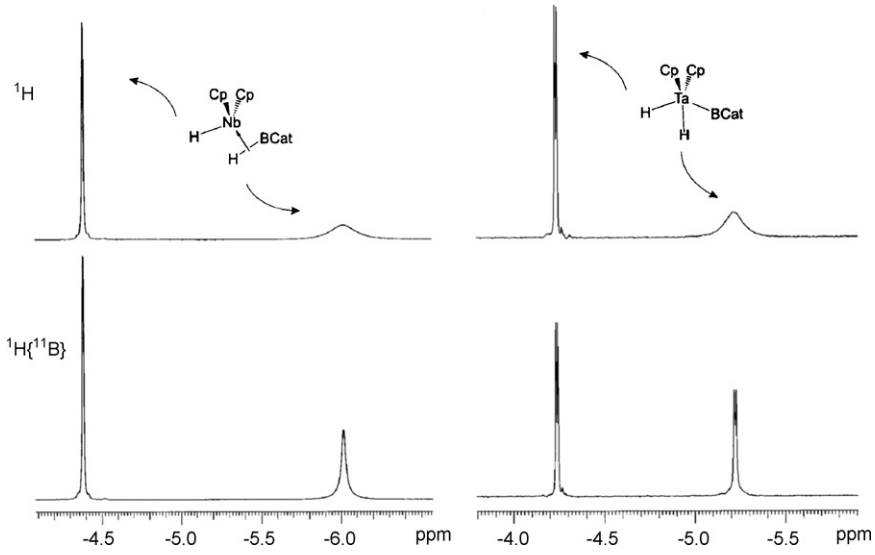

Fig. 13. ^{1}H and $^{1}H\{^{11}B\}$ for intermediate $Cp_2NbH(\eta^2\text{-HBcat})$ (left) at −20 °C and *exo*-$Cp_2TaH_2(Bcat)$ (right) at 20 °C. (Reprinted from Ref. [74] with permission of the American Chemical Society, Copyright 2007)

undergo hydrogen exchange processes with low activation barriers [71]. It is worth noting that a borohydride(silyl) isomer was optimized as the lowest minimum at the B3LYP/DFT level [72].

3.2. Niobium complexes

In 1994, niobium complexes incorporating catecholborane or 9-BBN (9-borabicyclo[3-3-1]nonane) were reported by Hartwig and De Gala [65]. Addition of the borane to Cp_2NbH_3 was performed at 55 °C in the case of catecholborane and at 20 °C in the case of 9-BBN. As shown in Fig. 12, the complexity results once more in the large number of possible coordination modes: hydrido-σ-B-H (**D**), *endo*-dihydrido(boryl) (**D_1**), *exo*-dihydrido(boryl) (**D_2**) or borohydride (**D_3**). On the basis of X-ray and NMR data the authors proposed a formulation **D_1** in the case of catecholborane and **D_3** in the case of 9-BBN. The complex $Cp_2NbH_2(Bcat)$ displays a broad signal at $\delta - 8.68$ and a ^{11}B NMR signal at δ 59. Isotopic labelling experiments revealed large perturbations by ^{1}H, ^{2}H and ^{11}B data. The large perturbations are in favour of a rapid equilibrium between structures **D_1** and **D_3**. The X-ray structure performed at −120 °C is in good agreement with a Nb(V) boryl formulation (structure **D_1**) as evidenced in particular by the very long B–H distances (1.69(5) Å).

A few years later, in 1997, a detailed study was performed by Smith and co-workers on the reactivity of $Cp^*_2MH(CH_2{=}CHR)$ (M = Nb, Ta; R = H, Me) with substituted catecholborane reagents [73]. M(V) structures appear to be dominant in this chemistry, however, the complex $Cp^*_2Nb(H_2Bcat\text{-}3\text{-}tBu)$ is better formulated as a Nb(III) complex with a borohydride coordination on the basis of X-ray data. The authors also observed large chemical shift perturbations upon isotopic labelling and it appears that the phenomenon is rather complex and might involve several equilibria. Finally in 1999, they found that upon reaction at −20 °C of *endo*/*exo*-$Cp_2NbH(CH_2{=}CHMe)$ with 1 equiv. of catecholborane, a new species was produced and identified as a niobium σ-catecholborane complex $Cp_2NbH(\eta^2\text{-HBcat})$ **D** [74]. At −20 °C, the ^{11}B NMR spectrum of intermediate **D** exhibits a signal at $\delta + 59$, thus downfield of free catecholborane ($\Delta\delta = +30$). The ^{1}H NMR displays a set of two hydride resonances: a sharp signal at $\delta - 4.40$ and a broad signal at $\delta - 6.00$ that sharpens upon ^{11}B decoupling (Fig. 13). For symmetry reasons, these data exclude the structure **D_1** displaying, as observed by Hartwig [65], one single hydride resonance at $\delta - 8.68$ in the ^{1}H NMR spectrum. For similar reasons, the borohydride coordination mode **D_3** that should additionally exhibit a more shielded resonance signal in the ^{11}B NMR was also discarded. The spectroscopic data were compared to that of *exo*-$Cp_2TaH_2(Bcat)$ that presents the same coordination mode than in **D_2** [66]. In the ^{11}B NMR, the *exo*-

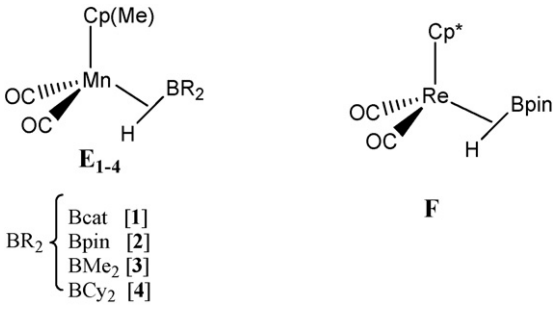

Fig. 14. Manganese and rhenium σ-borane complexes **E** and **F**.

$Cp_2TaH_2(Bcat)$ exhibits a signal at δ 64.7 located downfield of catecholborane ($\Delta\delta + 34.7$). In the ^1H NMR, the spectrum shows a temperature-independent sharp doublet at $\delta - 4.20$ with a $^2J_{HH}$ coupling constant of 5.6 Hz and a broad signal at $\delta - 5.17$ that sharpens into a well-resolved doublet upon ^{11}B decoupling (Fig. 13). In the case of complex **D**, it was not possible to measure any $^2J_{HH}$ from − 60 to 20 °C excluding the $\mathbf{D_2}$ coordination mode. The σ-B–H coordination mode in **D** was also revealed by isotopic labelling from *endo*/*exo*-$Cp_2NbH(CH_2{=}CHMe)$ and catB-D. The experiment resulted in the exclusive deuterium incorporation at $\delta - 6.21$ in the ^2H NMR spectrum gradually followed by a statistical redistribution between the positions corresponding to the two hydride resonances.

3.3. Manganese and rhenium complexes

Isolation of manganese and rhenium σ-BH complexes represents a milestone in the field of σ-borane coordination chemistry. In 2000, Hartwig and co-worker showed that σ-borane complexes were not restricted to early transition metals and moreover, for the first time, dialkylboranes were incorporated as σ-ligands in the coordination sphere of the metal [75]. Manganese complexes $\mathbf{E_{1–4}}$ were obtained by salt extrusion using $K[(MeCp)Mn(CO)_2H]$ and the corresponding halogenoboranes XBR_2 (X = Cl, Br; BR_2 = Bpin, Bcat, BMe_2, BCy_2) (Fig. 14). In the case of Bpin and Bcat complexes, another route involving photolysis of $(MeCp)Mn(CO)_3$ in the presence of pinacolborane or catecholborane was also possible, but the corresponding complexes were obtained in lower yields. Rhenium complex **F** resulted from the alcoholysis of *cis*-$Cp^*Re(CO)_2(Bpin)_2$ (Fig. 14). Complexes **E** and **F** were fully characterized by infrared, multinuclear NMR spectroscopy and their structure was rationalized by theoretical calculations. An X-ray structure was obtained in the case of σ-borane manganese complexes of catecholborane ($\mathbf{E_1}$), pinacolborane ($\mathbf{E_2}$) and dicyclohexylborane ($\mathbf{E_4}$).

The infrared vibrations observed between 1592 and 1606 cm^{-1} for **E** and at 1603 cm^{-1} for **F** were attributed to the Mn–H–B vibrator that is likely to be predominantly M–H in character. The B–H stretches are generally estimated to lie even lower in frequencies and of course much lower than in free monomeric boranes ($\nu_{catBH} = 2660\ cm^{-1}$, $\nu_{pinBH} = 2580\ cm^{-1}$ and calculated $\nu_{Me_2BH} = 2491\ cm^{-1}$). The IR-stretching frequencies of the carbonyl ligands are informative of the metal–borane synergetic electron transfer in **E**. The measured ν_{CO} stretching values suggest that dialkylboranes are stronger σ-donating and weaker π-accepting ligands than pinacolborane and catecholborane, respectively (see Table 3).

The values of the M–B distances in complexes $\mathbf{E_1}$, $\mathbf{E_2}$ and $\mathbf{E_4}$ are 2.083(2), 2.149(2) and 2.187(3) Å and are slightly longer than those in related iron boryl complexes $CpFe(CO)_2(Bcat)$ (1.959(6) Å) and $CpFe(CO)_2(BPh_2)$ (2.034(3) Å) [76]. They all contained extremely small H–Mn–B angles of 38.2°, 37.2° and 33.2° and the Mn–H bond distances of 1.57, 1.53 and 1.49 Å, respectively are very close to that of $K[(MeCp)Mn(CO)_2H]$ (1.54–1.56 Å) indicating a strong M–H interaction [77]. The B–H bond lengths of these complexes are, respectively 1.29, 1.31 and 1.24 Å. They are slightly longer than those calculated for B–H distances in the free boranes (1.184 Å in catecholborane, 1.190 Å in pinacolborane and 1.204 Å in Me_2BH) and compatible with complexes involving a σ-B–H bond [78].

For manganese compounds $\mathbf{E_{1–4}}$, the ^{11}B NMR clearly illustrates the nature of the borane incorporated in the complex. The $\mathbf{E_1}$ and $\mathbf{E_2}$ spectra exhibit a signal at δ 46 and δ 45, respectively, downfield of free catecholborane ($\Delta\delta + 17$) and free pinacolborane ($\Delta\delta + 17.6$ ppm). Similar spectroscopic data are observed with the rhenium σ-pinacolborane complex **F** ($\Delta\delta + 17$). In the case of $\mathbf{E_3}$ and $\mathbf{E_4}$, the ^{11}B NMR chemical shifts at $\delta + 101$ and $\delta + 104$ are also in agreement with the incorporation of a dialkylborane in the complex. In the ^1H NMR spectrum, complexes $\mathbf{E_{1–4}}$ and **F** exhibit a shielded hydride broad signal between $\delta - 17.06$ and $\delta - 11.06$ that sharpens upon ^{11}B decoupling (Fig. 15). In the case of $\mathbf{E_1}$ and $\mathbf{E_2}$, a direct J_{BH} coupling constant of 98 Hz and 88 Hz, respectively could be estimated for the first time. These values obtained by high temperature ^{11}B NMR experiments represent roughly half the value measured in the parent borane and ascertain a σ-borane formulation.

It is interesting to compare these data with those reported by Braunschweig et al. for similar manganese complexes with $BR_2 = BClE(SiMe_3)_3$ (E = Si, Ge) [79]. The $(MeCp)Mn(CO)_2H[BClE(SiMe_3)_3]$ complexes display similar

Table 3
IR and NMR data on manganese and rhenium complexes

	$\nu_{M–H–B}$ (cm^{-1})	$\nu_{s\,CO}$, $\nu_{as\,CO}$ (cm^{-1})	δ (^{11}B NMR) ($\Delta\delta$) (ppm)	δ (^1H NMR) (ppm)
$\mathbf{E_1}$	1606	1995, 1937	+46 (+17)	−14.46
$\mathbf{E_2}$	1603	1983, 1921	+45 (+17.6)	−15.66
$\mathbf{E_3}$	1592	1975, 1910	+101	−17.06
$\mathbf{E_4}$	1597	1967, 1901	+104	−16.96
F	1603	1981, 1924	+46 (+17)	−11.06

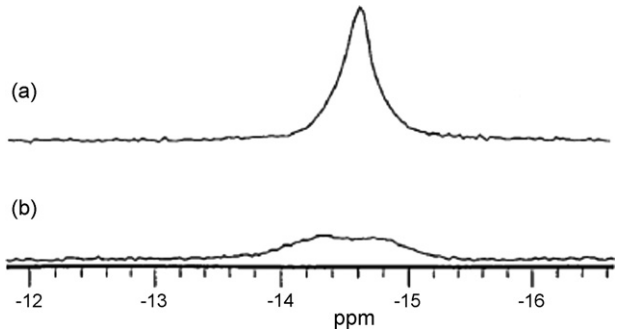

Fig. 15. ^{1}H NMR resonance of $\mathbf{E_1}$ at 25 °C (a) with and (b) without ^{11}B NMR decoupling. (Reprinted from Ref. [75] with permission of the American Chemical Society, Copyright 2007)

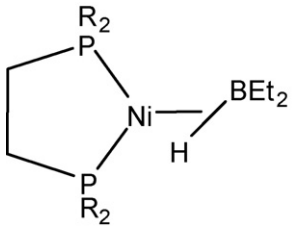

R = ^{i}Pr **[1]**, ^{t}Bu **[2]**, Cy **[3]**

$G_{1\text{-}3}$

Fig. 16. (dRpe)Ni(σ-HBEt$_2$) complexes **G**.

IR data and in particular the CO stretching frequencies at 1978, 1913 cm^{-1} (E = Si) and 1975, 1904 cm^{-1} (E = Ge) are comparable to those registered for $\mathbf{E_{3-4}}$. The X-ray structure of (MeCp)Mn(CO)$_2$H[BClSi(SiMe$_3$)$_3$] shows a Mn–B bond distance of 2.138(16) Å similar to that of $\mathbf{E_4}$ (2.187(3) Å) but due to the quality of the data, no information was available on parameters involving the hydride. The ^{11}B NMR resonances are similarly located downfield with a chemical shift of δ 105.2 (E = Si) and δ 105.8 (E = Ge). However, boryl iron complexes (MeCp)Fe(CO)$_2$[BClE(SiMe$_3$)$_3$] incorporating the same substituents at boron display more deshielded resonances (close to 140 ppm). Such a difference of chemical shifts is thus in favour of a residual H···B interaction in the manganese complexes leading formally to an increased coordination number at boron. The presence of a Mn–H–B bridge in solution is also indicated by the ^{1}H NMR spectra that exhibited a broad shielded signal at δ − 15.3 (E = Si) and δ − 15.03 ppm (E = Ge) that sharpened upon ^{11}B decoupling with a difference of line width of 15 and 5 Hz, respectively. The estimated coupling constant is in agreement with a hydrido(boryl)manganese formulation exhibiting a secondary interaction between the hydride and the boron atom [79].

In summary, in the case of $\mathbf{E_3}$ and $\mathbf{E_4}$ [75], the σ-borane formulation cannot be definitively established on the only basis of NMR spectroscopy and complementary data from X-ray analysis strengthen a σ-borane formulation. Such a formulation was recently ascertained by DFT calculations on the corresponding manganese and rhenium complexes, as reported by Pandey [78,80].

3.4. Nickel complexes

In 2005, Garcia and co-workers reported the first σ-borane nickel complexes by reaction of [(diphosphine)NiH]$_2$ with a mixture of triethylborane and Super-Hydride (LiBHEt$_3$) [81]. Three tetrasubstituted diphosphinoethane dRpe ligands (R = ^{i}Pr, ^{t}Bu, Cy) were used. The corresponding complexes (dRpe)Ni(σ-HBEt$_2$) ($\mathbf{G_{1-3}}$) were fully characterized by NMR spectroscopy and an X-ray structure was obtained in the case of $\mathbf{G_3}$ (Fig. 16). In $\mathbf{G_3}$, the metal–B, metal–H and B–H distances as well as the small H–M–B angle are similar to those in (MeCp)Mn(CO)$_2$(σ-HBCy$_2$) ($\mathbf{E_4}$), in agreement with the σ-coordination mode of the diethylborane to the nickel atom. Very recently, the boryl nickel complex (PNP)Ni(Bcat) was prepared and fully characterized (PNP = N[2-P(CHMe$_2$)$_2$-4-methylphenyl]$_2$) [82]. The Ni–B distance of 1.909(2) Å is significantly shorter than the σ-borane nickel complexes reported so far (see Table 4).

The ^{11}B NMR spectra of $\mathbf{G_{1-3}}$ show a signal between δ + 43 and δ + 48. These chemical shifts are surprisingly shielded compared to those of manganese σ-coordinated dialkylboranes [75] but remain moderately downfield of the dimeric (Et$_2$BH)$_2$ (δ + 37.72). The ^{1}H NMR spectra of $\mathbf{G_{1-3}}$ display a broad hydride resonance at *ca.* δ − 7. On the basis of these NMR data, it was difficult to exclude a hydrido(boryl) Ni(II) formulation rather than a σ-diethylborane complexation mode to a Ni(0) center. Further information given by the ^{31}P NMR was crucial to establish the most likely diethylborane coordination mode. The ^{31}P NMR spectra of $\mathbf{G_{1-3}}$ display a set of two slightly broadened asymmetric doublets, characteristic of two phosphorus atoms in a different environment (see Table 4). The $^{2}J_{PP}$ coupling constants are typical of Ni(0) complexes [83,84]. The hydrido(boryl) coordination mode can therefore be discarded at the benefit of a σ-diethylborane complexation.

3.5. Ruthenium complexes

The ruthenium σ-B–H complexes reported in the literature by Sabo-Etienne et al. are exclusively derived from the bis(dihydrogen) complex RuH$_2$(η^2-H$_2$)$_2$(PCy$_3$)$_2$ [85–87]. They are probably the most intriguing examples in terms of accessibility of various coordination modes. The presence of several hydrogen atoms in the coordination sphere of the metal makes these systems highly dynamic, with additional difficulties in obtaining reliable information in particular by NMR. The unique properties of σ-complexes and the tendency to be part of highly dynamic processes have allowed the establishment of the σ-CAM mechanism (σ-Complex Assisted Metathesis) as recently published by Perutz and Sabo-Etienne [3]. Such a concept is directly applicable to the catalytic borylation of alkanes extensively studied by Hartwig et al. [88].

Complex RuH[(μ-H)$_2$Bpin](η^2-HBpin)(PCy$_3$)$_2$ (**I**) was obtained in high yield by reaction of RuH$_2$(η^2-H$_2$)$_2$(PCy$_3$)$_2$ with an excess of pinacolborane at room temperature (Fig. 17). It incorporates two molecules of pinacolborane differently coordinated on the same ruthenium center: one σ-borane and one

Table 4
X-ray and NMR data on nickel complexes

	^{31}P NMR		δ ^{1}H NMR (ppm)	δ ^{11}B NMR (ppm)	M—B (Å)	M—H (Å)	B—H (Å)	H—M—B (°)
	δ (ppm)	$^{2}J_{PP}$ (Hz)						
G$_1$	77.5 and 66.4	67.8	−6.96 (b)	45.38				
G$_2$	95.9 and 84.1	63.9	−7.5 (b)	48				
G$_3$	72.2 and 58.3	77.8	−7.0 (b)	43.32	2.172(6)	1.47(5)	1.23(5)	32.8
E$_4$	–	–	−16.96 (b)	+104	2.187(3)	1.49(2)	1.24(2)	33.2(7)

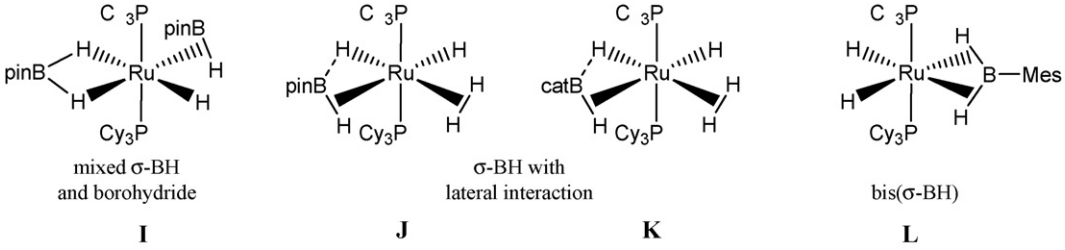

Fig. 17. Ruthenium borane σ-complexes **I**, **J**, **K** and **L**.

dihydroborate ligand. **I** was characterized by NMR spectroscopy and X-ray analysis [85,86]. The four coordination sites in the equatorial plane of the pseudo octahedral complex **I** are occupied by one hydride, one *exo*-σ-B–H pinacolborane and one dihydridopinacolborate ligated to the ruthenium centre by two hydrogen atoms. The Ru–B distance in the case of the σ-pinacolborane ligand (2.157(5) Å) is slightly shorter than that of the dihydridopinacolborate ligand (2.188(5) Å). The σ-B–H bond distance (1.35(3) Å) is elongated by *ca.* 16% relative to that of the calculated B–H bond distance of 1.17 Å in a free dialkoxyborane. It is shorter than the two B–H distances of the dihydridopinacolborate ligand (1.47(3) and 1.58(3) Å). The angle between the middle of [O,O], B and Ru for the coordinated dihydridopinacolborate (177.1°) is significantly different than for the σ-pinacolborane ligand (171.5°), probably the best criterion for the discrimination between the two modes [85,86]. The lowest minimum found by DFT calculations corresponds to the formulation with one σ-borane and one dihydroborate ligand, whereas a symmetrical isomer with two dihydroborate ligands was optimized 16 kJ mol^{-1} higher in energy on the potential energy surface [86].

The ^{11}B NMR spectrum at 293 K shows one single broad signal at δ 37.3 located downfield of free pinacolborane (δ 28.4). The room temperature ^{1}H NMR spectrum of **I** in the hydride region is featureless. However, at 233 K three well-resolved resonances in a 2:1:1 ratio are observed as a broad singlet at $\delta -11.4$, a sharp triplet at $\delta -8.03$ and a broad singlet at $\delta -7.13$ (Fig. 18). On the basis of the T_{1min} values (around 100 ms at 300 MHz for the three signals), the presence of a σ-dihydrogen ligand in **I** could be ruled out. The two broad signals that sharpen upon ^{11}B decoupling are attributed to the two bridging hydrogens of the dihydridoborate ($\delta -11.4$) and to the σ-B–H hydrogen atom ($\delta -7.13$). No coupling constant between ^{11}B and ^{1}H could be measured. The $^{2}J_{HP}$ coupling constant value of 25 Hz for the terminal hydride ($\delta -8.03$) coupled to the two phosphorus atoms is in agreement with a *cis*-coupling.

Complex $RuH_2(\eta^2\text{-HBpin})(\eta^2\text{-H}_2)(PCy_3)_2$ (**J**) (Fig. 17) was observed by reaction of $RuH_2(\eta^2\text{-H}_2)_2(PCy_3)_2$ with a stoichiometric amount of pinacolborane at room temperature or by exposing complex **I** under an atmosphere of dihydrogen [86]. The best method for the isolation of **J** was to react $RuH_2(\eta^2\text{-H}_2)_2(PCy_3)_2$ with pinB–Bpin under thermal conditions (80 °C). Complex **J** was characterized by NMR spectroscopy, by X-ray analysis at 90 K and the structure was also rationalized by theoretical calculations. The four coordination sites in the equatorial plane of the pseudo octahedral structure are occupied by two hydrides in *cis* position, one *endo*-σ-B–H pinacolborane and one σ-dihydrogen ligand perpendicular to the equatorial plane. The quality of the X-ray data allowed the location of the dif-

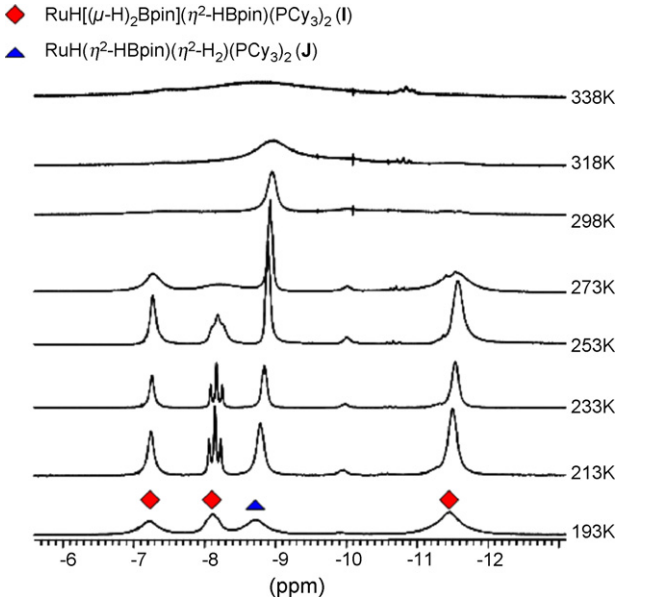

Fig. 18. ^{1}H NMR spectra in the hydride region at variable temperatures of a mixture of **I** and **J**.

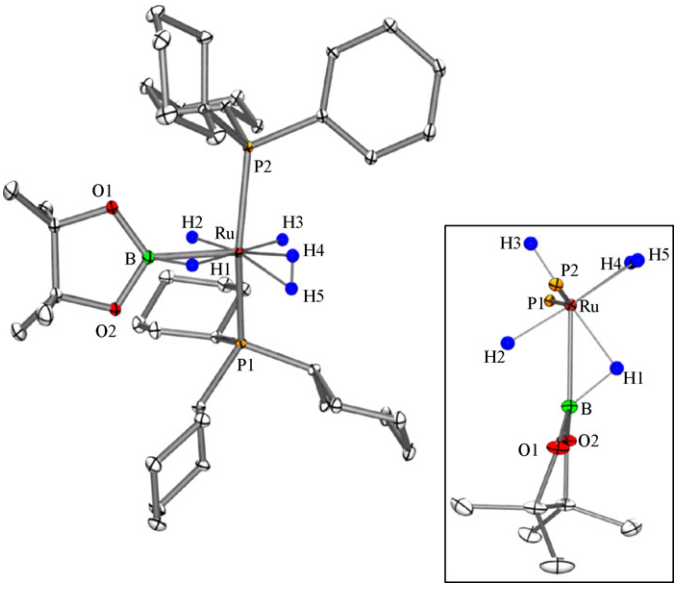

Fig. 19. Ortep drawing of $RuH_2(\eta^2\text{-HBpin})(\eta^2\text{-}H_2)(PCy_3)_2$ (**J**).

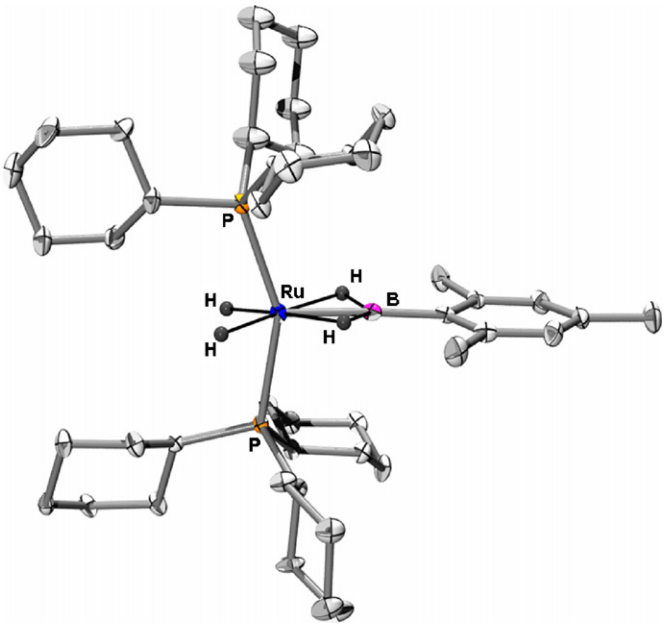

Fig. 20. Ortep drawing of $RuH_2(\eta^2{:}\eta^2\text{-}H_2BMes)(PCy_3)_2$ (**L**).

ferent hydrogen atoms and unexpectedly the dihydrogen ligand was found in a perpendicular plane to the other hydrogen atoms, a situation quite uncommon in polyhydride ruthenium chemistry (Fig. 19). Such a position results from the presence of two σ-ligands, σ-dihydrogen and σ-borane, which need in order to be stabilized to favour back-donation from the metal. Competition between the two σ-ligands is avoided by a position in orthogonal planes. This was also highlighted by a theoretical analysis. The H–H distance of 0.79(3) Å shows that the dihydrogen ligand is only slightly activated. The Ru–B distance of 2.173(2) Å is slightly longer than that of the σ-pinacolborane ligand in complex **I**. With 1.30(2) Å, the σ-B–H distance represents a normal elongation for a σ-borane complex. The angle between the middle [O,O], B and Ru (170°) is close to the corresponding angle (171.5°) in **I**. The B···H distance of 1.89(2) Å between the boron atom and the closest hydride is much longer than the B–H distances in the dihydroborate ligand in **I** (1.47 and 1.58 Å) but is in favour of a small hydride/boron lateral interaction.

The ^{11}B NMR spectrum at 293 K shows one single broad signal at δ 35.8, located slightly downfield of free pinacolborane and very close to **I**. The ^{1}H NMR spectrum displays in the high-field region only one broad signal at $\delta - 8.83$ corresponding to five hydrides in fast exchange (Fig. 18). No decoalescence was observed even at 183 K. The T_{1min} value of 40 ms at 253 K (300 MHz) is in agreement with the presence of a σ-H_2 ligand. It is interesting to compare those data with other ruthenium complexes incorporating a pinacolboryl ligand. For example, in the case of the hydrido(boryl) complex $RuH(Bpin)(C_2H_4)(PCy_3)_2$ the boron signal displays the same chemical shift (δ ^{11}B 34.6) whereas the hydride resonates as a triplet at $\delta - 5.77$ ($J_{P-H} = 35$ Hz) [89].

Complex $RuH_2(\eta^2\text{-HBcat})(\eta^2\text{-}H_2)(PCy_3)_2$ (**K**) (Fig. 17) was obtained in moderate yield by reaction of $RuH_2(\eta^2\text{-}H_2)_2(PCy_3)_2$ with a stoichiometric amount of catecholborane at room temperature [86]. It was characterized by NMR spectroscopy, by X-ray analysis at 100 K and the structure was rationalized by theoretical calculations. Comparable structural features with those of **J** were obtained. The σ-B–H bond distance of 1.24(2) Å is also in agreement with a σ-catecholborane formulation. The B···H distance of 1.60 Å between the boron and the closest hydride is shorter than in **J** and reveals a stronger lateral interaction probably due to an increased Lewis acidity of the involved borane. This trend is verified in the case of 9-BBN activation since the corresponding dihydridorate complex $RuH[(\mu\text{-}H)_2BBN](\eta^2\text{-}H_2)(PCy_3)_2$ was exclusively obtained. The ^{11}B NMR spectrum of **K** shows a broad signal at δ 35.8 located downfield of free catecholborane ($\Delta\delta + 7$). In the ^{1}H NMR, the hydrides are all in fast exchange even at 183 K and a single broad resonance is obtained at $\delta - 8.48$. The integration is in agreement with the incorporation of one catecholborane group in the coordination sphere of the metal. The T_{1min} value of 47 ms at 198 K (300 MHz) indicates like for **J** the presence of a σ-H_2 ligand. In the cases of **J** and **K**, the NMR data appeared less conclusive. Their formulation as σ-borane complexes was best ascertained by X-ray diffraction and DFT analysis.

Complex $RuH_2(\eta^2{:}\eta^2\text{-}H_2BMes)(PCy_3)_2$ (**L**) is the first example of one borane bound to the metal center through two geminated σ-B–H bonds (Figs. 17 and 20) [87]. It was obtained in excellent yield by reaction of $RuH_2(\eta^2\text{-}H_2)_2(PCy_3)_2$ with a stoichiometric amount of dimeric mesitylborane $(H_2BMes)_2$ or from $RuHCl(\eta^2\text{-}H_2)(PCy_3)_2$ in the presence of lithium mesitylborohydride. It was characterized by NMR spectroscopy, and its structure was determined by X-ray diffraction at 100 K (Fig. 20) and was also analyzed by theoretical calculations. The four coordination sites in the equatorial plane of the pseudo octahedral structure are occupied by two hydrides in *cis* position and one bis(σ-B–H) coordinated mesitylborane. The Ru–B distance of 1.938(4) Å is the shortest Ru–B bond ever reported, much shorter than the sum of the covalent radii (2.09 Å) suggesting an interaction between the metal center and the boron atom. The

B–H bond distances (1.24(3) and 1.29(3) Å) are less than 10% elongated by comparison to the calculated B–H bond distances of 1.197 Å in a free monomeric mesitylborane showing only a slight activation. The ^{11}B NMR spectrum at 293 K shows a broad signal at δ 58 located downfield of starting dimeric mesitylborane (δ 22). The ^{1}H NMR spectrum of **L** exhibits at 296 K in the hydride region two resonances in a 1:1 ratio. The broad singlet at $\delta - 5.90$ that sharpens upon boron decoupling is attributed to the two hydrogen atoms attached to boron, whereas the triplet at $\delta - 11.05$ that collapses into a singlet upon phosphorus decoupling ($^{2}J_{PH} = 25.2$ Hz) is in agreement with a *cis* coupling of two hydrides with two equivalent phosphorus atoms. The T_{1min} measurements on the hydride resonances rule out the presence of any σ-H_2 ligand in **L**. No direct coupling constant between ^{11}B and ^{1}H could be measured. The formulation as a bis-σ-borane complex is best ascertained by X-ray diffraction and DFT analysis. The coordination of the two geminated σ-B–H bonds involves σ-donation to the ruthenium and π-back-donation from the ruthenium to the vacant p orbital of boron.

4. Conclusion

The present selection of results on σ-silane and σ-borane complexes illustrates the benefits of using NMR as a technique allowing in particular discrimination between a σ-formulation and the corresponding product of oxidative addition. However, none of the common parameters deriving from NMR analysis can be used as a unique probe to ascertain a σ-formulation. Chemical shift values demonstrate the incorporation of the silane (borane) into the coordination sphere of the metal but are not informative on the real nature of the bonding mode. One can expect to define more precisely the situation by obtaining ^{29}Si and ^{11}B NMR parameters (chemical shifts and coupling constants) but very few data are still available. Coupling constant values tend to be much more informative but again care must be taken on a direct analysis. Variable temperature studies often give insight into exchange processes, but in polyhydride systems it is often difficult to block the exchange pathways. We have seen over the years the benefits of combining X-ray and DFT analysis to ascertain a better location of hydrogen atoms. We believe that NMR and DFT data will become more and more complementary, as chemical shift and coupling constant values become now computationally calculated with a better accuracy [90,91].

The limits of NMR analysis we have evidenced in this review should not overcome the extreme benefit one can gain from this technique, which still remains one of the best method for the characterization of organometallic complexes. Substantial progress in ^{29}Si and ^{11}B NMR acquisition has been made and this area should also benefit from the tremendous improvement seen recently in solid state NMR [92,93].

Acknowledgements

We would like to thank the CNRS for the financial support of research carried out in our laboratory. S.S.-E. warmly thanks her co-workers for their valuable contributions to the work that is described in this article.

References

[1] G.J. Kubas, Metal Dihydrogen and σ-Bond Complexes, Kluwer Academic/Plenum Publishers, New York, 2001.
[2] G.J. Kubas, Catal. Lett. 104 (2005) 79.
[3] R.N. Perutz, S. Sabo-Etienne, Angew. Chem. Int. Ed. 46 (2007) 2578.
[4] G.J. Kubas, R.R. Ryan, B.I. Swanson, P.J. Vergamini, H.J. Wasserman, J. Am. Chem. Soc. 106 (1984) 451.
[5] P.G. Jessop, R.H. Morris, Coordin. Chem. Rev. 121 (1992) 155.
[6] R.H. Crabtree, Angew. Chem. Int. Ed. Engl. 32 (1993) 789.
[7] D.M. Heinekey, W.J.J. Oldham, Chem. Rev. 93 (1993) 913.
[8] S. Sabo-Etienne, B. Chaudret, Coordin. Chem. Rev. 178–180 (1998) 381.
[9] D.M. Heinekey, A. Lledos, J.M. Lluch, Chem. Soc. Rev. 33 (2004) 175.
[10] G.J. Kubas, Chem. Rev. 107 (2007) 4152.
[11] F. Maseras, A. Lledos, E. Clot, O. Eisenstein, Chem. Rev. 100 (2000) 601.
[12] M. Grellier, L. Vendier, B. Chaudret, A. Albinati, S. Rizzato, S. Mason, S. Sabo-Etienne, J. Am. Chem. Soc. 127 (2005) 17592.
[13] W.H. Lam, S. Shimada, A.S. Batsanov, Z. Lin, T.B. Marder, J.A. Cowan, J.A.K. Howard, S.A. Mason, G.J. McIntyre, Organometallics 22 (2003) 4557.
[14] S. Lachaize, S. Sabo-Etienne, Eur. J. Inorg. Chem. (2006) 2115.
[15] S. Lachaize, S. Sabo-Etienne, Eur. J. Inorg. Chem. (2006) 4697.
[16] J.K. Hoyano, M. Elder, W.A.G. Graham, J. Am. Chem. Soc. 91 (1969) 4568.
[17] E. Colomer, R.J.P. Corriu, C. Marzin, A. Vioux, Inorg. Chem. 21 (1982) 368.
[18] U. Schubert, Adv. Organomet. Chem. 30 (1990) 151.
[19] J.Y. Corey, J. Braddock-Wilking, Chem. Rev. 99 (1999) 175.
[20] I. Atheaux, B. Donnadieu, V. Rodriguez, S. Sabo-Etienne, B. Chaudret, K. Hussein, J.C. Barthelat, J. Am. Chem. Soc. 122 (2000) 5664.
[21] R. Ben Said, K. Hussein, J.-C. Barthelat, I. Atheaux, S. Sabo-Etienne, M. Grellier, B. Donnadieu, B. Chaudret, Dalton Trans. (2003) 4139.
[22] X.-L. Luo, G.J. Kubas, C.J. Bums, J.C. Bryan, C.J. Unkefer, J. Am. Chem. Soc. 117 (1995) 1159.
[23] W. Jetz, W.A.G. Graham, Inorg. Chem. 10 (1971) 4.
[24] U. Schubert, G. Scholz, J. Mueller, K. Ackermann, B. Woerle, R.F.D. Stansfield, J. Organomet. Chem. 306 (1986) 303.
[25] U. Schubert, B. Wörle, P. Jandik, Angew. Chem. Int. Ed. 20 (1982) 695.
[26] D.L. Lichtenberger, A. Rai-Chaudhuri, Organometallics 9 (1990) 1686.
[27] D.L. Lichtenberger, A. Rai-Chaudhuri, J. Am. Chem. Soc. 112 (1990) 2492.
[28] R. Karch, U. Schubert, Inorg. Chim. Acta 259 (1997) 151.
[29] U. Schubert, K. Ackermann, B. Woerle, J. Am. Chem. Soc. 106 (1984) 7378.
[30] U. Schubert, K. Ackermann, G. Kraft, B. Woerle, Z. Naturforsch. B 38 (1983) 1488.
[31] G.I. Nikonov, Organometallics 22 (2003) 1597.
[32] D.L. Lichtenberger, Organometallics 22 (2003) 1599.
[33] W. Scherer, G. Eickerling, M. Tafipolsky, G.S. McGrady, P. Sirsch, N.P. Chatterton, Chem. Commun. (2006) 2986.
[34] N.M. Yardy, F.R. Lemke, L. Brammer, Organometallics 20 (2001) 5670.
[35] V.K. Dioumaev, B.R. Yoo, L.J. Procopio, P.J. Carroll, D.H. Berry, J. Am. Chem. Soc. 125 (2003) 8936.
[36] K. Hübler, U. Hübler, W.R. Roper, P. Schwerdtfeger, L.J. Wright, Chem. Eur. J. 3 (1997) 1608.
[37] M. Mohlen, C.E.F. Rickard, W.R. Roper, D.M. Salter, L.J. Wright, J. Organomet. Chem. 593–594 (2000) 458.
[38] K. Hussein, C.J. Marsden, J.C. Barthelat, V. Rodriguez, S. Conejero, S. Sabo-Etienne, B. Donnadieu, B. Chaudret, Chem. Commun. (1999) 1315.
[39] G.I. Nikonov, Angew. Chem. Int. Ed. Engl. 40 (2001) 3353.
[40] V.K. Dioumaev, L.J. Procopio, P.J. Carroll, D.H. Berry, J. Am. Chem. Soc. 125 (2003) 8043.
[41] S. Sabo-Etienne, M. Hernandez, G. Chung, B. Chaudret, New J. Chem. 18 (1994) 175.

[42] S. Lachaize, S. Sabo-Etienne, B. Donnadieu, B. Chaudret, Chem. Commun. (2003) 214.
[43] F. Delpech, S. Sabo-Etienne, B. Chaudret, J.-C. Daran, J. Am. Chem. Soc. 119 (1997) 3167.
[44] F. Delpech, S. Sabo-Etienne, J.C. Daran, B. Chaudret, K. Hussein, C.J. Marsden, J.C. Barthelat, J. Am. Chem. Soc. 121 (1999) 6668.
[45] I. Atheaux, F. Delpech, B. Donnadieu, S. Sabo-Etienne, B. Chaudret, K. Hussein, J.C. Barthelat, T. Braun, S.B. Duckett, R.N. Perutz, Organometallics 21 (2002) 5347.
[46] J. Yin, J. Klosin, K.A. Abboud, W.M. Jones, J. Am. Chem. Soc. 117 (1995) 3298.
[47] S. Shimada, M. Tanaka, M. Shiro, Angew. Chem. Int. Ed. 35 (1996) 1856.
[48] T. Ayed, J.-C. Barthelat, B. Tangour, C. Pradère, B. Donnadieu, M. Grellier, S. Sabo-Etienne, Organometallics 24 (2005) 3824.
[49] S. Lachaize, Ph.D., Université Toulouse III – Paul Sabatier, France, 2004.
[50] S. Aldridge, D.L. Coombs, Coordin. Chem. Rev. 248 (2004) 535.
[51] H. Braunschweig, C. Kollann, D. Rais, Angew. Chem. Int. Ed. 45 (2006) 5254.
[52] M. Ingleson, N.J. Patmore, G.D. Ruggiero, C.G. Frost, M.F. Mahon, M.C. Willis, A.S. Weller, Organometallics 20 (2001) 4434.
[53] G.J. Irvine, M.J.G. Lesley, T.B. Marder, N.C. Norman, C.R. Rice, E.G. Robins, W.R. Roper, G.R. Whittell, L.J. Wright, Chem. Rev. 98 (1998) 2685.
[54] M. Shimoi, S. Nagai, M. Ichikawa, Y. Kawano, K. Katoh, M. Uruichi, H. Ogino, J. Am. Chem. Soc. 121 (1999) 11704.
[55] M.R. Smith III, Prog. Inorg. Chem. 48 (1999) 505.
[56] O. Volkov, R. Macias, N.P. Rath, L. Barton, Inorg. Chem. 41 (2002) 5837.
[57] T. Yasue, Y. Kawano, M. Shimoi, Angew. Chem. Int. Ed. Engl. 42 (2003) 1727.
[58] J.F. Hartwig, C.N. Muhoro, X. He, O. Eisenstein, R. Bosque, F. Maseras, J. Am. Chem. Soc. 118 (1996) 10936.
[59] H.C. Brown, M. Zaidlewicz, Organic Syntheses via Boranes, Aldrich Chemical Company, Inc., Milwaukee, 2001.
[60] C.D. Entwistle, T.B. Marder, P.S. Smith, J.A.K. Howard, M.A. Fox, S.A. Mason, J. Organomet. Chem. 680 (2003) 165.
[61] H. Beall, C.H. Bushweller, Chem. Rev. 73 (1973) 465.
[62] T.J. Marks, L.A. Shimp, J. Am. Chem. Soc. 94 (1972) 1542.
[63] D. Reed, Boron NMR, in: D.M. Grand, R.K. Harris (Eds.), Encyclopedia of Nuclear Magnetic Resonance, John Wiley and Sons, 1996.
[64] C.N. Muhoro, X. He, J.F. Hartwig, J. Am. Chem. Soc. 121 (1999) 5033.
[65] J.F. Hartwig, S.R. De Gala, J. Am. Chem. Soc. 116 (1994) 3661.
[66] D.R. Lantero, D.H. Motry, D.L. Ward, M.R. Smith III, J. Am. Chem. Soc. 116 (1994) 10811.
[67] J.F. Hartwig, C.N. Muhoro, Organometallics 19 (2000) 30.
[68] C.N. Muhoro, J.F. Hartwig, Angew. Chem. Int. Ed. Engl. 36 (1997) 1510.
[69] C.N. Iverson, M.R. Smith Jr., J. Am. Chem. Soc. 121 (1999) 7696.
[70] S.A. Westcott, N.J. Taylor, T.B. Marder, R.T. Baker, N.J. Jones, J.C. Calabrese, Chem. Commun. (1991) 304.
[71] T.J. Marks, J.R. Kolb, Chem. Rev. 77 (1977) 263.
[72] D. Liu, K.C. Lam, Z. Lin, Organometallics 22 (2003) 2827.
[73] D.R. Lantero, D.L. Ward, M.R. Smith III, J. Am. Chem. Soc. 119 (1997) 9699.
[74] D.R. Lantero, S.L. Miller, J.-Y. Cho, D.L. Ward, M.R. Smith III, Organometallics 18 (1999) 235.
[75] S. Schlecht, J.F. Hartwig, J. Am. Chem. Soc. 122 (2000) 9435.
[76] J.F. Hartwig, S. Huber, J. Am. Chem. Soc. 115 (1993) 4908.
[77] N.P. Chatterton, G. Guilera, G.S. McGrady, Organometallics 23 (2004) 1165.
[78] K.K. Pandey, J. Organomet. Chem. 692 (2007) 1997.
[79] H. Braunschweig, M. Colling, K. Kolann, U. Englert, J. Chem. Soc., Dalton Trans. (2002) 2289.
[80] K.K. Pandey, J. Mol. Struct. Theochem. 807 (2007) 61.
[81] M.G. Crestani, M. Muñoz-Hernandez, A. Arévalo, A. Acosta-Ramirez, J.J. Garcia, J. Am. Chem. Soc. 127 (2005) 18066.
[82] D. Adhikari, J.C. Huffman, D.J. Mindiola, Chem. Commun. (2007) 4489.
[83] J.J. Garcia, A. Arevalo, N.M. Brunkan, W.D. Jones, Organometallics 23 (2004) 3997.
[84] J.J. Garcia, N.M. Brunkan, W.D. Jones, J. Am. Chem. Soc. 124 (2002) 9547.
[85] V. Montiel-Palma, M. Lumbierres, B. Donnadieu, S. Sabo-Etienne, B. Chaudret, J. Am. Chem. Soc. 124 (2002) 5624.
[86] S. Lachaize, K. Essalah, V. Montiel-Palma, L. Vendier, B. Chaudret, J.C. Barthelat, S. Sabo-Etienne, Organometallics 24 (2005) 2935.
[87] G. Alcaraz, E. Clot, U. Helmstedt, L. Vendier, S. Sabo-Etienne, J. Am. Chem. Soc. 129 (2007) 8704.
[88] J.F. Hartwig, K.S. Cook, M. Hapke, C.D. Incarvito, Y. Fan, C.E. Webster, M.B. Hall, J. Am. Chem. Soc. 127 (2005) 2538.
[89] A. Caballero, S. Sabo-Etienne, Organometallics 26 (2007) 1191.
[90] T. Ziegler, J. Autschbach, Chem. Rev. 105 (2005) 2695.
[91] A. Toner, J. Matthes, S. Grundemann, H.H. Limbach, B. Chaudret, E. Clot, S. Sabo-Etienne, PNAS 104 (2007) 6945.
[92] M.J. Duer, Solid-State NMR Spectroscopy. Principles and Applications, Blackwell Science Ltd., Oxford, 2002.
[93] P. Avenier, M. Taoufik, A. Lesage, A. Baudouin, X. Solans-Monfort, A. De Mallmann, L. Veyre, J.M. Basset, O. Eisenstein, L. Emsley, E.A. Quadrelli, Science 317 (2007) 1056.